Modeling the Dual-Slope Behavior of in-Quad EL-FEXT in Twisted Pair Quad Cables

Rob F. M. van den Brink

***Abstract*— It is well known that the ratio between received crosstalk and received signal in telephony cabling increases with the frequency until both levels become about equal. Transmission systems like VDSL and G.fast are designed to cope with that. But the awareness that the increase of EL-FEXT (equal level - far end cross talk) becomes much stronger above a certain frequency (increases with 40 dB instead of 20 dB per decade) was raised only recently in ITU and BBF standardization bodies for G.fast. This second order effect became known under the name "dual slope" effect, was initially not well understood, and resulted in a number of conjectured explanations. This paper demonstrates that this second order effect in far end crosstalk between opposite wire pairs in the same quad is deterministic in nature. It is caused by the interaction of the twist in a quad and its metallic surroundings (e.g., shield). The twist of these quads reduces this second order crosstalk effect significantly, but what remains causes a slope of 40 dB/decade. This paper shows via a model that this second order effect scales linearly with the cable length and twist length, and validates that via measurements. It quantifies how sensitive this effect is to cable design parameters like twist length and capacitance to shield. In addition, an extension is proposed to a commonly used simplified system model for describing the far end cross talk as a function of the frequency and cable length.**

***Index Terms*— Twisted pair (quad) cables, crosstalk, EL-FEXT, transmission line matrix methods, subscriber loops, DSL**

I. Introduction

DIGITAL subscriber line (DSL) modems, aimed for the next generation broadband via copper [1], are designed to transmit their signals through multi-pair telephony cables under noisy stress conditions. This noise originates via crosstalk from other DSL systems using other wire pairs in the same cable. Most of this crosstalk can be eliminated by proper vectoring techniques [2], a technique that has become common within DSL systems, and required by G.fast [3] and VDSL [4] standards (VDSL=Very high speed DSL). But these crosstalk levels can even exceed the levels of DSL signals above some break-frequency at given cable length [5], [6]. This puts strong demands on vectoring engines to handle these high crosstalk levels as well. G.fast can transmit signals up to 106 MHz (and in future up to 212 MHz) and recent versions of VDSL up to 35 MHz. Using these frequencies required the development of more advanced models for twisted pair cables up to hundreds of MHz [7]–[9].

Manuscript received January 20, 2016; revised May 23, 2016 and November 20 2016; accepted February 3, 2017. Date of publication February 14, 2017; date of current version May 13, 2017. The associate editor coordinating the review of this paper and approving it for publication was M. Guenach.

The author is with TNO, 2509 JE Den Haag, Netherlands (e-mail: Rob.vandenBrink@tno.nl).

Color versions of one or more of the figures in this paper are available online at http://ieeexplore.ieee.org.

Digital Object Identifier 10.1109/TCOMM.2017.2669032

Legacy models on crosstalk [10], [11] assume that the ratio between far-end crosstalk and signals transmitted via the direct channel (the equal level - far end crosstalk or just EL-FEXT) increases in frequency with a slope of 20 dB/decade and increases in length with the square-root of the cable length. But more recent measurements focused on higher frequencies revealed a dual-slope behavior of the EL-FEXT [5], [6], [12] showing a second order crosstalk effect of 40 dB/decade as well. This second order effect has a significant impact on the usability of higher frequency bands by DSL systems and their vectoring engines. This is because the effect doubles the slope of the EL-FEXT above some break frequency, and becomes dominant thereafter. Break frequencies as low as 2 MHz have been observed as well.

This behavior was raised [5], [12] in ITU-T SG15/Q4, which is the standardization body for VDSL and G.fast, and was soon confirmed by others [13]–[19]. It was clearly visible between wire pairs in the same quad of several multi-quad cables, and observed to be cable-type and quad dependent. This effect was not so visible or sometimes invisible in the available cable measurements between different quads.

Initially the cause was not well-understood, and this resulted in a number of conjectured explanations for the dual slope effect, as summarized in [20]:sect5.2. One conjecture [20] is the normal, expected behavior of coupled transmission lines. Another conjecture [20] is that it is the "upward" ramp of a resonance which takes place beyond 106 MHz. This resonance is the result of parasitic mutual inductance and mutual capacitance. A third conjecture [20] is that it is the result of propagation through the various "phantom" or alternate paths that can couple two loops.

The phenomenological dependency on coupling length was suggested in [15], [18] on the basis of available measurements. Although [18] relates the dual slope effect to the twist of the wires and the shield, that paper did not quantify the effect via modeling. But they could successfully use the deterministic nature of the effect to suppress the 40 dB/decade slope by alternating the twist orientation over the cable length (partially left or right twist orientation). The more recent TR-285 [21], [22] from Broadband Forum is illustrative for the state of the art on cable models, and refers to the dual slope effect as just "experimental observations". It models (in A.2.3.4) the EL-FEXT with just two straight lines (one for each slope) and models the length dependency of both the first and second order effect equally, and proportionally with $\sqrt{L}$. It also describes a full multi-port cable model, and phrases (in section B.1.5.4) the opposite: that length dependency of the in-quad crosstalk is "in general" proportional to the length L. In spite

of the capabilities of that advanced model, TR-285 [21] does not detail on the cause of both slopes and on the fact that they both scale differently with the loop length. As a result, a good understanding on how the characteristics of this second order effect relates to various cable characteristic is currently lacking.

The present paper shows via modeling and experiments that the cause of the second order crosstalk effect of in-quad FEXT is different and independent from the well-known first order effect and will also scale differently with the cable length. The presence of both effects gives the EL-FEXT its dual slope behavior. This second order effect is caused by deterministic variations in the geometry of the wiring with respect to their shield (an/or metallic surroundings), and can even be present in the absence of random perturbations (causing the first order effect).

As opposed to a brute force modeling approach in [21], [23], [24], the present paper is restricted to the modeling of a single quad (4 wires with a common twist) with respect to a shield. The aim is to gain understanding on the physical mechanism causing the observed behavior. A full description on how multiple quads in the same cable will interact with each other is kept out-of scope of this paper. This simplifies complex matters significantly and allows for exploring the most striking dependencies of the dual slope effect in various dimensions. Section II starts with a brief summary of measurements to show how this second order effect is visible in EL-FEXT between opposite wire pairs in the same quad. The existence of this crosstalk effect between different quads of a multi-quad cable is a bit inconclusive from available measurements and that question is considered as out-of-scope of this paper. Section III elaborates on a full eight-port model of four wires in a quad to study the impact of twisting four wires in the vicinity of a shield to gain understanding. Section IV to VI provide novel material, by building further on cascaded models and explores the dependency of the effect in various dimensions. Section IV shows how reliable this approach is, section V analyses how the second order effect depends on design parameters such as twist length, and section VI analyses how it scales with the loop length. Section VII validates our predictions that the second order EL-FEXT behavior scales proportionally with the loop length and twist length. The eight-port model is quite reliable but often too complicated for simple system calculations on modem performance. Therefore we propose in section VIII an extension to a commonly used simplified model for EL-FEXT to cover the first and second slope and their length-dependencies as well. A preliminary version of this paper is meanwhile contributed to the members of ITU-T SG15/Q4 as [25] and to the members of Broadband Forum as [26]–[28] to assist the relevant standardization bodies with further understanding on the dual slope effect.

II. Appearance of EL-FEXT in Real Cables

To illustrate the dual slope effect, we selected a characterization [6] of a multi-pair telephony cable, 378 m in length and winded on a drum, where the wires are organized in groups

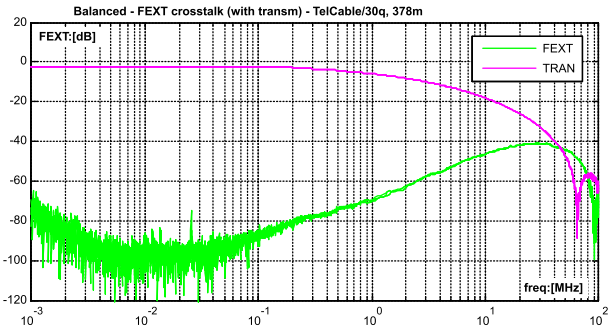

Fig. 1. Transmission and FEXT, measured in both directions of a 378 m multi quad telephony cable.

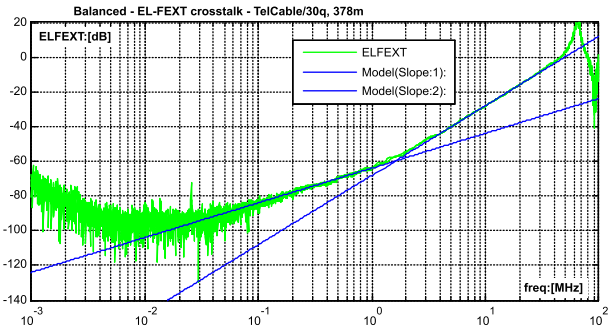

Fig. 2. The dual slope behavior of the magnitude of the EL-FEXT (20 and 40 dB/decade).

of four wires (30 twisted quads in total, similar to figure 4) and where the cable has a common shield. Measurements were performed directly on the individual wires (using the shield as common) by means of an 8-port network analyzer, without balanced transformers and with full 8-port correction of systematic measurement errors [6], [29].

The measured s-parameters represent all possible direct transmission, reflection and crosstalk values of four individual wires with respect to a common ground (an 8-port has 64 of these values). But DSL modems are using these wires in pairs, and are connected to them via balanced transformers. Therefore the differential mode transmission and crosstalk through or between these wires pair were calculated from these 64 numbers. The results are shown in figure 1 to 3.

A. Observations on Crosstalk

Figure 1 shows two curves, the upper curve "TRAN" representing the measured balanced transmission in a wire pair of a quad, and the lower curve "FEXT" representing the far end crosstalk to that wire pair. These two quantities are equal to (differential mode) s-parameters of the quad in the cable. More precisely, when the near and far-end ports of a first wire pair is labeled as "1" and "2', and of a second wire pair as "3" and "4", then the (forward) transmission equals s_{21} for the first wire pair and s_{43} for the second wire pair (s_{yx} represents the scatter parameter from port "x" to "y"). The (forward) FEXT equals to s_{23} and s_{41} respectively. So figure 1 contains four in stead of two curves, but this is hardly visible since they overlap.

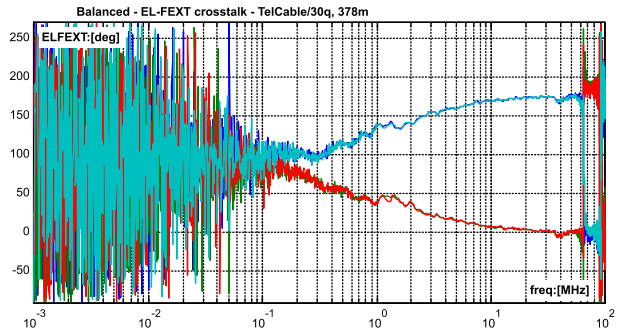

Fig. 3. The phases of both forward EL-FEXT transfers in a quad converge to opposite signs between 1 and 60 MHz.

The FEXT increases with the frequency, and beyond about 50 MHz the crosstalk levels are even higher than the direct transmission levels.

Figure 2 shows a curve "ELFEXT" which is the (complex) ratio between two transfer functions, labeled as "FEXT" and "TRAN" in figure 1. More precisely, the EL-FEXT of the first wire pair is s_{23}/s_{21} and of the second wire pair s_{41}/s_{43}. Figure 2 shows the magnitude (in dB) of this complex ratio, as well as two additional asymptotic lines, labeled as "slope 1" (of 20 dB/decade) and "slope 2" (of 40 dB/decade). These lines are to highlight the dual slope effect of this EL-FEXT curve.

The asymptotic lines cross each other near 2 MHz, but that break frequency is cable, quad and length dependent. So in this example the second slope becomes dominant above about 2 MHz and affects almost the full VDSL band. This dependency is clearly visible in measurements on different cable types as reported in [5]. Values ranging from 1 MHz to 15 MHz have been observed. Above 60 MHz, the EL-FEXT "resonates" around 0 dB. This is typical behavior as observed in many cables, is well-predictable by our model in section III (and shown in figure 7), but not simply related to a single quantifier. It is not really related to noise and/or randomness and could be referred to as "a complex composition of various higher order effects".

Figure 3 shows two curves, each of them representing the measured phase of the EL-FEXT to a first wire pair and to a second wire pair in the same quad. Above about 2 MHz, the measured crosstalk raises above the noise floor of the setup and the two phases split-up and converge to opposite signs. That behavior is typical within quads where the dual-slope effect is clearly visible.

Above 60 MHz the phase gives the impression to become random, but this is mainly due to rapid phase variations by the above mentioned "higher order effects". These variations are mainly deterministic in nature, start near the first "resonating" peak of figure 2, and can reasonably be described by the model introduced in section III-A. The same phase curves are also shown in figure 8 with a linear scale (and combined with the model) and illustrate this effect even better.

B. Description of First and Second Order Effects

The cause of the first order slope (20 dB/decade) is well known [10], [11]. If the centers of four wires in a quad are perfectly positioned at the corners of a square, and balanced signals are using opposite wires as a pair, then all crosstalk to the other wire pair in the same quad will be zero due to perfect symmetry. But the smallest deviation from that perfection will already result in some residual crosstalk. This causes the well-known first order crosstalk effect, since real cables will always have small imperfections in the symmetry of their quads, which are also randomly distributed along the cable length. Twisting does not really help against this first order crosstalk within the same quad; it helps minimizing the crosstalk between wire pairs from other quads.

But there is also another crosstalk effect, as will be discussed in the rest of this paper via simulation. If the geometry in the quad is of perfect shape, but the quad is in the vicinity of a shield (or conductive surroundings like other quads) then the electrical symmetry within the quad is disturbed since each wire may have a slightly different capacitive coupling to that shield. This can be minimized by twisting the full quad, and after many twists each wire has on average the same capacitance to shield. The tighter the quad is twisted the better this works and the less disturbance the shield will have on the electrical symmetry. But there will always be a residue, causing a small amount of extra crosstalk, and our model quantifies that this deterministic effect causes the second order slope (40 dB/decade).

III. Modeling Approach

The wire pairs in a multi quad cable are organized in groups of four wires, as shown in figure 4, and surrounded by a common shield. Each pair (1-2) or (3-4) of opposite wires is being used in a balanced mode. When the geometry of such a quad is a perfect square, and when the quad is far away from the shield and other quads, then the symmetry will cause that the crosstalk from one balanced pair (1-2) to the other balance pair (3-4) in the same quad is zero. But this is not the case in practice, for instance when the quad is in the vicinity of a shield. Then each wire has an additional capacitance to that shield (and to other quads) as well, as shown in the circuit equivalent of figure 4.

This capacitance is not equal for each wire and thus deteriorates the overall symmetry of the quad. This is one of the reasons why quads are twisted so that each wire approaches the shield as often as the other three over each twist length. This makes all wire capacities to shield equal on average, restores the balance on average and reduces the overall crosstalk significantly.

To model this twisting effect, we consider the cable as a long cascade of very short cable sections of four wire structures. If the length of each section is short enough (compared to the twist length) then they can be assumed as piece-wise uniform over its length. Each section may have different uniformity but this will be repetitive if the wires are regularly twisted. One can obtain the transfer functions of interest by treating each uniform section with four wires as an 8-port (using the shield as common), by cascading them all over the full cable length as 8-ports, and by extracting from that cascade the overall balanced transfers of the wire pairs.

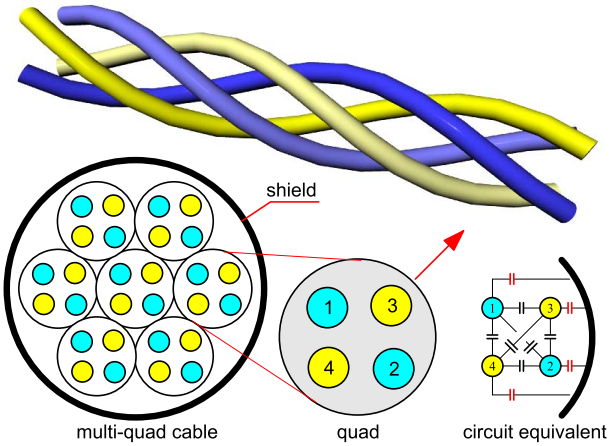

Fig. 4. A multi-quad cable is organized in groups of four wires positioned in a square, and each quad is twisted many times over its full length. Opposite wires (1-2) and (3-4), are used for (balanced) transmission, and each wire has a capacitance to all the other wires and to the common shield.

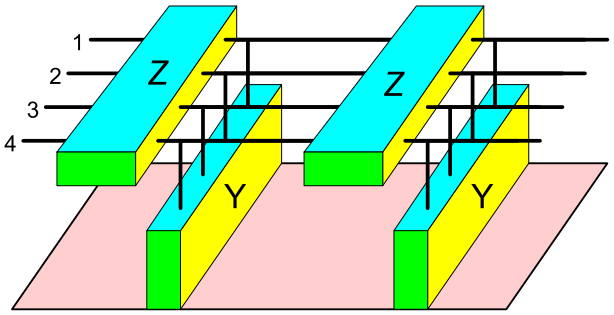

Fig. 5. An alternating cascade of infinite thin networks can represent a uniform cable.

A. Modeling Uniform Cable Sections

A complete modeling of each uniform cable section can be obtained via the well-known multi-conductor transmission line equations [30]:ch3, [8], [21], [23], [24]. When z denotes the longitudinal position in this cable structure, then the vectors of voltages $\mathbf{U}$ and currents $\mathbf{I}$ at each position z are given by the matrix collection in eq. 1.

$$\begin{aligned} \frac{\partial}{\partial z}\mathbf{U}(z) &= -\mathbf{Z}_s \cdot \mathbf{I}(z) \\ \frac{\partial}{\partial z}\mathbf{I}(z) &= -\mathbf{Y}_p \cdot \mathbf{U}(z) \end{aligned} \tag{1}$$

In these expressions, $\mathbf{Z}_s$ is the series impedance matrix per unit length and $\mathbf{Y}_p$ the shunt admittance matrix. If we split them into their real and imaginary parts we may phrase them as $\mathbf{Z}_s = \mathbf{R}_s + j\omega\mathbf{L}_s$ and $\mathbf{Y}_p = \mathbf{G}_p + j\omega\mathbf{C}_p$. Note that all these matrices are in principle non-zero and frequency dependent. This description can be thought of as an alternating cascade of infinite thin (inductive) series networks and (capacitive) shunt networks, as depicted in figure 5.

The series impedance matrix $\mathbf{Z_S}$ is dominantly inductive in nature representing the series inductance (per unit length) of individual wires and their mutual magnetic coupling. By adding series resistors we can account for the cable loss. The shunt admittance matrix $\mathbf{Y}_p$ is dominantly capacitive in nature representing all capacitive coupling (per unit length) between the wires and the shield.

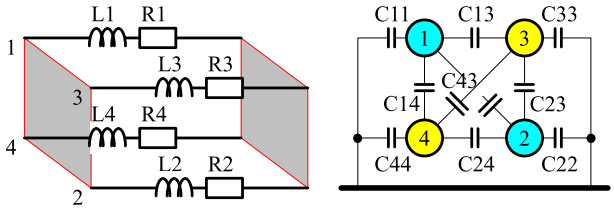

Fig. 6. The Z-matrix is (mainly) inductive in nature and the Y-matrix is capacitive in nature.

Figure 6 shows a circuit diagram with lumped elements of this concept when a uniform 4-wire structure is surrounded by a shield. This concept can be generalized for more wires. If losses are involved then the circuit diagram can be extended with (low) resistors in series with the inductors and by adding a small loss-angle to the capacitors. In principle, none of these lumped elements are zero nor frequency in-dependent.

Cable modeling is essentially the finding of parametric expressions to evaluate the matrices $\mathbf{Z_S}$ and $\mathbf{Y}_p$ as function of the frequency. Once these matrices are modeled, a full multi-port cable model of a uniform section is simply the evaluation of multi-port s-parameters from a pair $\{\mathbf{Z_S}, \mathbf{Y}_p\}$ via known calculation methods [21], [24], [30]. Similarly, a cascade of uniform sections is modeled via additional cascade calculations with multi-port s-parameters [30]. These modeled s-parameters are to be the same as those that have been measured directly on the cable, otherwise the model is inadequate. From this point the evaluation of cable properties such as EL-FEXT are the same as those used after measurements.

The aim of this paper is not to make the best possible cable model that handles all cable details very well, but to make the simplest model that is adequate enough to raise understanding on the cause of the dual slope effect. One such simplification is assuming that all dielectric losses are zero, that both $\mathbf{C}_p$ and $\mathbf{L}_s$ are frequency-independent and that all cable loss is caused by series resistance. To model however cable loss sufficiently fair over a wide frequency interval, each series resistance should be modeled with a strong frequency dependency to address additional losses caused by the skin effect in each wire.

Effort on two-port cable modeling up to hundreds of MHz [7]–[9] has learned that this simplification is not entirely true but that the capacitance is rather constant over a wide frequency interval, the inductance converges roughly to a constant value above a few hundreds of kHz, and that dielectric losses are small compared to resistive losses. Extracted matrix values for $\mathbf{C}_p$ and $\mathbf{L}_s$ from multi-port cable measurements [6] show a similar behavior over a sufficiently wide frequency interval. The error we make by using the above mentioned simplification is irrelevant for understanding the dual-slope effect, since the resulting multi-port cable model can still offer a sufficiently good match between model and measurements (as will be shown in figure 7).

B. Modeling the Matrices of Uniform Sections

1) Capacitance Matrix $\mathbf{C}_p$: To model $\mathbf{Y}_p$ from this example structure we therefore assume $\mathbf{G}_p = 0$ and assume $\mathbf{C}_p$

to be frequency-independent. In other words, we assume only ideal lumped capacitors between the wires and/or shield, where $C_{rk} = C_{kr}$ denotes the lumped capacitance per unit length between wire r and k, and C_{kk} between wire k and the common shield. By transforming this lumped circuit description into its Y-parameter representation, we obtain the desired (symmetric) $\mathbf{Y}_p$ for a 4-wire structure, as expressed in eq. 2.

$$\mathbf{Y}_p = j\omega \cdot \mathbf{C}_p = j\omega \cdot \begin{bmatrix} \sum C_1 & -C_{12} & -C_{13} & -C_{14} \\ -C_{21} & \sum C_2 & -C_{23} & -C_{24} \\ -C_{31} & -C_{32} & \sum C_3 & -C_{34} \\ -C_{41} & -C_{42} & -C_{43} & \sum C_4 \end{bmatrix} \quad (2)$$

Where $\Sigma C_r = C_{r1} + C_{r2} + C_{r3} + C_{r4} = C_{1r} + C_{2r} + C_{3r} + C_{4r}$.

2) Inductance Matrix $\mathbf{L_s}$*:* To model the imaginary part of $\mathbf{Z}_s$ from our example structure we assume $\mathbf{L_s}$ to be frequency-independent (the measurements reported in [6] show that this is a fair approximation), and its real part by a simple frequency-dependency for $\mathbf{R}_s$. In other words we assume for $\mathbf{L}_s$ only ideal lumped inductors that are all magnetically coupled, and for $\mathbf{R}_s$ resistors in series with these inductors. Similarly to $\mathbf{C}_p$ we can model $\mathbf{L}_s$ independently by assuming lumped inductance and coupling values. However this approach can easily result in cable models predicting properties that are physically impossible. Therefore it is often more convenient to evaluate $\mathbf{L}_s$ via a detour.

Lets therefore assume another (hypothetical) wiring structure where all copper is exactly the same as the real one but where all insulation around that copper is assumed to be fully absent. In other words: as if all conductors are suddenly floating in vacuum. Such a hypothetical wiring structure has different properties and the inductance and capacitance matrices will change accordingly from $\{\mathbf{L}_s, \mathbf{C}_p\}$ to $\{\mathbf{L}_{s0}, \mathbf{C}_{p0}\}$. What we gain from that approach is (a) that now $\mathbf{L}_{s0}$ can easily be derived from $\mathbf{C}_{p0}$, (b) that $\mathbf{L}_s$ can easily be derived from $\mathbf{L}_{s0}$ and that (c) $\mathbf{C}_{p0}$ is relatively simple to estimate from the values of $\mathbf{C}_p$.

Lets clarify that step by step. The first step (a) is possible since the free-space matrix relation $\mathbf{L}_{s0} \times \mathbf{C}_{p0} = \mathbb{I}/c_0^2$ holds for this hypothetical structure. See [30]:eq3.37, [8]:eq4. In this expression, matrix $\mathbb{I}$ refers to the identity matrix and constant $c_0 = 3 \cdot 10^8$ m/s refers to the speed of light in vacuum. Such a simple relation does not hold between $\mathbf{L}_s$ and $\mathbf{C}_p$. since the dielectric between the wire pairs is not homogeneous (insulation has gaps between the wires, filled with air and/or gel). Step (b) is possible since $\mathbf{L}_s$ and $\mathbf{L}_{s0}$ have equal values since the magnetic properties of the actual and hypothetical structure are the same (only the dielectric properties have changed). Step (c) is a bit more complicated. If all insulation has vanished then all lumped capacitances reduce in value by a factor roughly equal to the dielectric constant(s) of the used insulation material. Typically a value somewhere between about 2.0 and 4.0 for real telephony cables. Estimating realistic values for these scaling factors is less critical than directly estimating realistic values for the mutual inductances in $\mathbf{L}_s$, and this makes the use of above detour less error-prone and therefore more convenient.

TABLE I
NOMINAL PARAMETER VALUES, TO SIMULATE A SECTION

$C_{11} \approx C_{22} \approx C_{33} \approx C_{44}$	C_c	10	pF/m
$C_{31} \approx C_{42} \approx C_{32} \approx C_{41}$	C_p	22	pF/m
$C_{21} \approx C_{43}$	C_q	9.5	pF/m
$\varepsilon_{11} \approx \varepsilon_{22} \approx \varepsilon_{33} \approx \varepsilon_{44}$	ε_c	3.3	
$\varepsilon_{13} \approx \varepsilon_{42} \approx \varepsilon_{32} \approx \varepsilon_{41}$	ε_p	2.5	
$\varepsilon_{21} \approx \varepsilon_{43}$	ε_q	3.1	
R_{s0}	R_{s0}	0.0863	Ω/m
R_{s1}	R_{s1}	0.130	Ω/m
R_{s2}	R_{s2}	0.018	Ω/m

In conclusion, when ϵ_{rk} represents the scaling for lumped capacitance C_{rk} to $C_{rk0} = C_{rk}/\epsilon_{rk}$, then we can create $\mathbf{L}_s$ via expression (3). And since $\epsilon_{rk} = \epsilon_{kr}$ and $C_{rk} = C_{kr}$, only three independent ϵ values are to be estimated for a perfect symmetrical quad structure to extract $\mathbf{L}_s$ from $\mathbf{C}_p$.

$$\mathbf{L}_s = \frac{1}{c_0^2} \cdot \begin{bmatrix} \sum CE_1 & -C_{12}/\epsilon_{12} & -C_{13}/\epsilon_{13} & -C_{14}/\epsilon_{14} \\ -C_{21}/\epsilon_{21} & \sum CE_2 & -C_{23}/\epsilon_{23} & -C_{24}/\epsilon_{24} \\ -C_{31}/\epsilon_{31} & -C_{32}/\epsilon_{32} & \sum CE_3 & -C_{34}/\epsilon_{34} \\ -C_{41}/\epsilon_{41} & -C_{42}/\epsilon_{42} & -C_{43}/\epsilon_{43} & \sum CE_4 \end{bmatrix}^{-1} \quad (3)$$

Where $\Sigma CE_r = C_{r1}/\epsilon_{r1} + C_{r2}/\epsilon_{r2} + C_{r3}/\epsilon_{r3} + C_{r4}/\epsilon_{r4}$.

3) Resistance Matrix $\mathbf{R}_s$ *:* To complete the modeling of $\mathbf{Z}_s$ with its real part, we also assume $\mathbf{R}_s$ as the result of 4 lumped resistors, in series with the four lumped inductors in $\mathbf{L}_s$. This simplifies $\mathbf{R}_s$ into a diagonal matrix since the dielectric is assumed to act as perfect insulator. These resistors are to be frequency-dependent to account for the skin-effect in the wires, and when modeling such a curve in a pure mathematical manner then a simple truncated series expansion in $\sqrt{\omega}$ can represent this dependency quite well. If each wire r adds an equal series resistance to each inductance, then this diagonal matrix $\mathbf{R}_s$ becomes as expressed in eq. 4.

$$\mathbf{R}_s = \left(R_{s0} + \sqrt{\frac{\omega}{\omega_0}} \cdot R_{s1} + \frac{\omega}{\omega_0} \cdot R_{s2} + \cdots \right) \cdot \begin{bmatrix} 1 & 0 & 0 & 0 \\ 0 & 1 & 0 & 0 \\ 0 & 0 & 1 & 0 \\ 0 & 0 & 0 & 1 \end{bmatrix} \quad (4)$$

Where $R_{s0}, R_{s1}, \ldots$ are all constants and $\omega_0 = 2\pi \cdot 1MHz$.

4) Assumed Parameter Values: The nominal values in table I are chosen to offer a good match between the cable measurements in the figures 1, 2 and 3, and what the model predicts. This match will be demonstrated in figure 7 and 8. These nominal values are found in an iterative manner, starting from estimated values for C and ϵ. These estimations were taken from [6], where both the cable measurements as well as the extracted values for $\mathbf{C}$ and $\mathbf{L}$ were reported for this particular cable. These first estimates gave already a fair match and could be manually improved by tuning the values and inspecting the match between the measurements and what the model predicts in terms of s-parameters.

Nominal values for $\{R_{s0}, R_{s1}, R_{s2}, \ldots\}$ were found in an iterative manner. A starting value for R_{s0} was obtained via

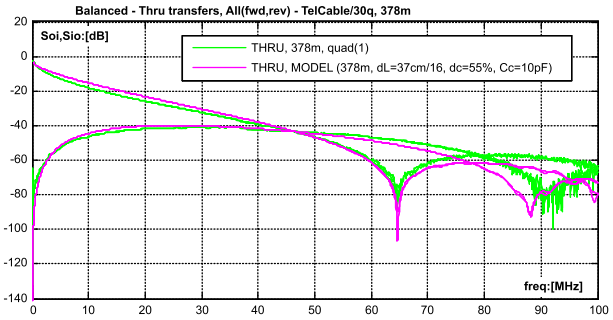

Fig. 7. Match of transmission and FEXT magnitudes, between model and measurement.

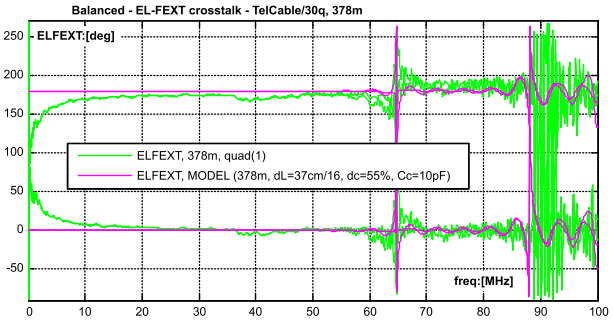

Fig. 8. Match of EL-FEXT phase, between model and measurement.

low-frequency measurements of series resistance and the other values were initially assumed to be zero. They were improved via manual iteration, by comparing the measured cable loss with the loss predicted via these numbers. A fair match could be achieved (see figure 7 and 8) with only the first three terms of the series expansion of $\mathbf{R}_s$ as non-zero. The rest of the polynomial expansion was truncated.

5) Multi-Port Parameters: With only 9 nominal values per unit length, a full multi-port parameter description of a symmetric and uniform line can be evaluated from the matrices $\mathbf{Z}_s$ and $\mathbf{Y}_p$. To add twisting to this multi-port model, an additional set of 3 numbers is required, as outlined in section III-C.

These matrices $\mathbf{Z}_s$ and $\mathbf{Y}_p$ are subsequently transformed into single wire s-parameters for the full cable, using known methods as described for instance in [30] and from that the mixed mode s-parameters for the balanced wire pairs.

C. Modeling the Twist in the Quad

The full cable however is not uniform because the twist in the wires causes the distance between each wire and the shield to vary with the z position in that cable. As a result the capacity from wire to shield varies regularly from a minimum to a maximum value, and back. We have approximated this over a full twist length by cascading n uniform but slightly different sections, where $n \geqslant 4$. The four capacitance values from the wires to the shield vary gradually with the position of each section while all other values in table I are kept at their nominal value. The theoretical capacitance between two flat metallic plates is roughly inversely proportional with the distance d. This property is used here to estimate how the capacitance between wire and shield varies with the distance.

TABLE II
PARAMETER VALUES USED TO SIMULATE THE TWISTING

Sections per twist	"n"	n	16
Twist length	"dL"	ΔL	37 cm
Shield unbalance	"dc"	Δ_c	0.55

The twist varies this distance in a harmonic manner over a full twist length ΔL, and therefore this variance in segment k has been modeled as shown in eq. 5.

$$\begin{aligned} C_{11} &= C_c/\left(1+\Delta_c \cdot \sin(2\pi \cdot k/n)\right) \\ C_{22} &= C_c/\left(1-\Delta_c \cdot \sin(2\pi \cdot k/n)\right) \\ C_{33} &= C_c/\left(1+\Delta_c \cdot \cos(2\pi \cdot k/n)\right) \\ C_{44} &= C_c/\left(1-\Delta_c \cdot \cos(2\pi \cdot k/n)\right) \end{aligned} \tag{5}$$

In these expressions, C_c is a nominal capacitance, Δ_c a chosen "shield unbalance" factor, n the number of steps per twist, k an integer index of the section, $z{=}\frac{k}{n} \cdot \Delta L$ the longitudinal position in the cable after k sections and ΔL the twist length. The values for n, ΔL and Δ_c in our simulation are taken from table II, and for C_c from table I. The full cable can subsequently be approximated by repeating this cascade as often as needed for creating the full cable length (over 16000 sections in our example cable). This is a brute force approach, but allows us to analyze various cable properties.

IV. SIMULATION ACCURACY

A. Match Between Model and Data

The modeling approach of the previous chapter in combination with the nominal values from table I and II offers a close prediction of the measured cable properties of our example cable. Figure 7 illustrates how close the magnitudes of measured and modeled transmission and far-end crosstalk can be with above mentioned values. It shows two measured and two modeled curves, one representing the transmission through a wire pair and the other representing the far-end cross talk between two wire pairs of the same quad. Both show a good match up to high frequencies and even the dip in the transmission around 65 MHz is well predicted by the model. The match between the curves in figure 7 becomes weaker for the highest frequencies, and is most pronounced by the deviation of the measured and modeled dip around 90 MHz. This small deviation is not a surprise since all values of the inductance and capacitance matrices have been modeled as frequency in-dependent (to keep the model as simple as possible), while multi-port measurements on this cable have shown [6] that both vary a bit with the frequency. Since all geometric imperfections of the quad were ignored, except for the twist and for a shield, these dips are apparently caused by the interaction between twist and shield.

Figure 8 shows the match between measured and modeled phase of the two EL-FEXT curves of a quad in forward direction. Our model predicts a phase of 0 and 180 degrees between the two EL-FEXT curves in forward direction and this holds for the frequencies above about 2 MHz (from where the second order effect dominates the crosstalk) until

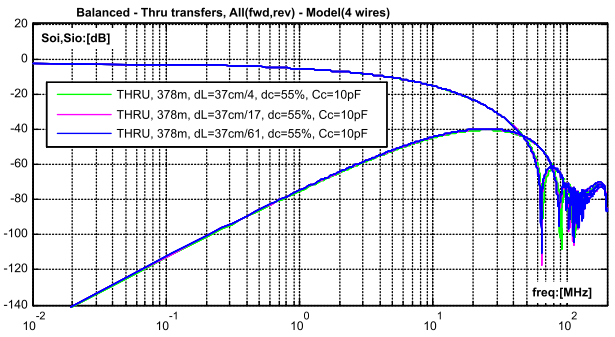

Fig. 9. A simulation with only 4 steps per twist offers similar result as a simulation with 17 or 61 steps per twist. This illustrates that modeling a twist with only 4 steps per twist is often adequate.

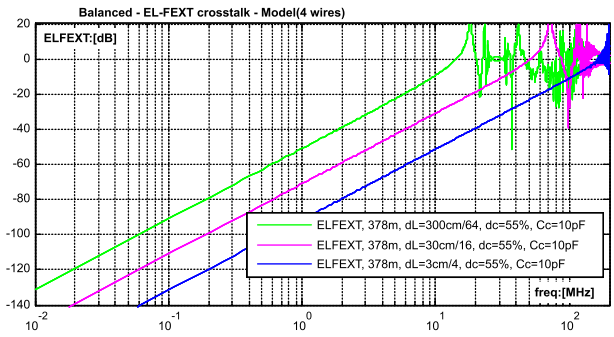

Fig. 10. An increase of twist-length by a factor 10 increases the EL-FEXT by 20 dB. The second-order EL-FEXT scales proportionally with the twist length.

about 60 MHz (from where the EL-FEXT has approached its asymptotic value of 0 dB).

B. Impact of Steps Per Twist

To verify if the number n of homogeneous sections per twist is large enough, we simulated the same cable length several times with an increasing number n. Figure 9 shows the simulated transfer and FEXT crosstalk of a 378 m loop when we evaluate it for n=4, 17 and 61 sections per twist respectively. This figure illustrates that this number hardly influences the result and that even a simulation with just 4 sections per twist is adequate.

V. Predictions on Geometric-Dependency

Now the model has shown to be reliable, we can use it to predict the dependency of EL-FEXT (ratio between FEXT and direct transmission) on several design parameters of the cable. This includes the impact of designing a cable with a tighter/looser twist or smaller/bigger variations of wire capacity to shield, or the impact of that nominal capacitance.

A. Dependency on Twist Length ΔL

Figure 10 shows the simulated results on the same loop when the twist length ΔL varies from 3 to 300 cm. It shows three curves, each of them representing EL-FEXT at another twist length (distance of a full 360° turn of a quad). All other parameters are assumed to be at the nominal values of table I and II, so the quad is assumed to be perfectly symmetrical causing the first order slope (20 dB/decade) to be absent.

A first observation is that the slope of the second order EL-FEXT is accurately 40 dB/dec over a very wide frequency interval. Another observation is that when the twist becomes tighter, the magnitude of this second order effect drops. A decrease of twist length by a factor 10 results in 20 dB reduction of EL-FEXT. In other words: the EL-FEXT is proportional to the twist length in this region. In addition, when the second-order EL-FEXT approaches the value one, the "rippling" around that asymptotic value becomes seemingly random in appearance, since in this region it is quite sensitive to small changes in assumptions.

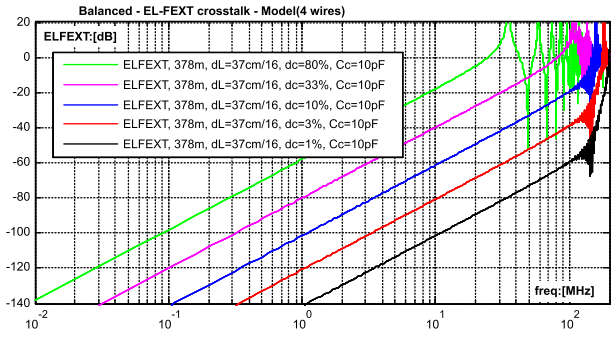

Fig. 11. An increase of the unbalance in capacity to shield by a factor 10 increases the EL-FEXT by 40 dB.

B. Dependency on Shield Unbalance Δ_C

Figure 11 shows various EL-FEXT curves for the same loop length when the variation between minimum and maximum capacitance from wire to shield changes. It shows five curves where the shield unbalance Δ_c (as defined in table II) varies in steps from 1% to 80%. This shield unbalance appeared to have a significant impact on the second order EL-FEXT. Each increase by a factor 10 causes 40 dB increase in EL-FEXT. But in all cases the slope of the second order EL-FEXT remains accurately 40 dB/decade over a very wide frequency interval.

C. Dependency on Capacitance to Shield

The nominal capacitance between wire and shield is not only determined by the nominal distance but also by the wire gauge and the dielectric in-between. Figure 12 shows four curves of EL-FEXT, where the (nominal) capacity C_c varies from 0.1 pF to 100 pF. And all other parameters remain as defined in table I and II. This time, the EL-FEXT does not change linearly with this capacity. In our example, it changes about 20 dB from 0.1 to 1 pF, 18 dB from 1 to 10 pF and about 9 dB from 10 to 100 pF.

VI. Predictions on Length-Dependency

The overall EL-FEXT increases with the cable length and is a combination of both the first and the second order behavior of the EL-FEXT. Both have a different origin and there is no reason why both should scale equally with the cable length.

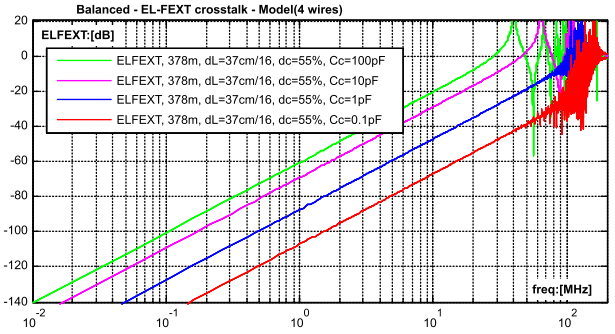

Fig. 12. An increase of the nominal capacitance between wire and shield increases the EL-FEXT in a non-linear way.

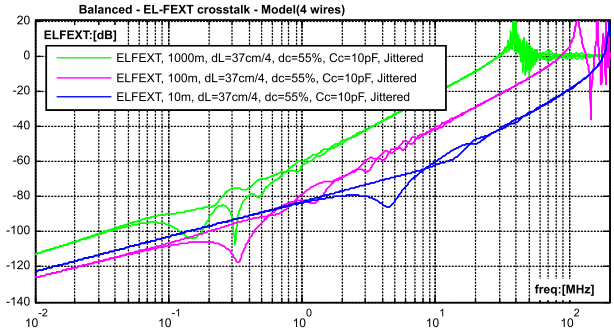

Fig. 13. Simulated EL-FEXT magnitude as function of the loop length. The second -order EL-FEXT scales proportionally with the loop length.

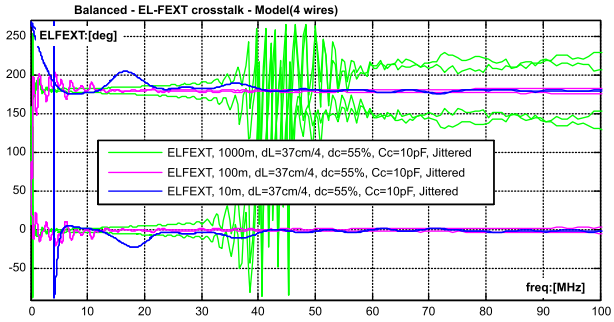

Fig. 14. Simulated EL-FEXT phase as function of the loop length; they have opposite values in the same direction.

The origin of the first order crosstalk effect is well known and originates from random perturbations of the geometry [10], [11]. When the four wires are positioned in a perfect square, and this symmetry would not have been disturbed by a shield, then there will be no crosstalk. But in practice this perfection is easily disturbed by random variation of the position and size of each wire. This causes crosstalk. Moreover, it is also well known that the associated EL-FEXT scales with the root of the cable length (in a statistical sense) and with a slope of 20 dB/decade [10], [11].

The second order effect even occurs in the full absence of these random perturbations, and even when the wires are positioned in a perfect square. The presence of a shield can disturb the electrical balance between opposite wires and the presence of twisting can reduce this effect significantly but not completely. This all makes the second order effect more deterministic in nature, and makes it plausible that it increases proportionally with the cable length.

In practice, however, there will always be a combination of both the first and the second order effect, and both will scale differently with the cable length. To prove the statements of the previous section, we will make our model more realistic and cover both the first and the second order effect in the same simulation. We have added random variation of capacitances around their nominal values, and apply these random changes to each small (uniform) section of the cascade calculation. This required a brute force cascade calculation of a huge number of uniform sections, where the capacitors C_p and C_q are randomly "jittered" for about 1% around their deterministic values in table I. This causes a first order behavior of the EL-FEXT, in superposition with the second order behavior.

Figure 13 shows three times two EL-FEXT curves (for both wire pairs) from these brute force simulations, where the loop length varies in steps from 10 m via 100 m to 1000 m. The low frequency part of these curves (below about 1 MHz) shows that the first order EL-FEXT increases a bit random with the loop length. Roughly 10 dB when the length increases by a factor 10. This demonstrates that the first order EL-FEXT increases roughly proportionally with the square root of the cable length, but this increase holds only in a statistical sense (averaged over many of these experiments). The mid-band frequencies of these curves (between about 1 and 100 MHz) show that the second order EL-FEXT increases consistently by 20 dB when the length increases by a factor 10. This demonstrates the expected linear increase of the EL-FEXT with the loop length. At higher frequencies, all EL-FEXT curves meander almost randomly around the value of 0 dB.

Figure 14 shows two groups of curves, representing the phase of the two forward EL-FEXT curves in the same quad. In all cases they have roughly opposite values around 0 and 180 degrees over the frequency band where the second order effect dominates.

VII. Validation of Predictions

To validate our predictions that the second order EL-FEXT scales proportionally with the loop length as well as with the twist length, we measured a multi-quad cable with six quads. It is a high quality rigid telephony cable, being used in the last copper drop of the Dutch access network, that can be buried directly in the ground. The wire structure is very similar to the one drawn in figure 4, with the difference that all six quads are positioned in a circle around a center core of plastic. The cable is shielded with a solid sheet of metal around those six quads (connected to "common" of the measurement setup) and has a second shield around the first one (isolated from the first one, but not connected). To observe the length-dependency of EL-FEXT, the length of the cable was subsequently cut-back from 104 m via 32 m to 10 m.

Figure 15 shows the two (forward) in-quad EL-FEXT curves of a single quad "A", measured at the three different loop lengths. The figure is for each length combined with a straight line, defined as $K_{XF2} \cdot (L/L_0) \cdot (\omega/\omega_0)^2$, where L is the loop

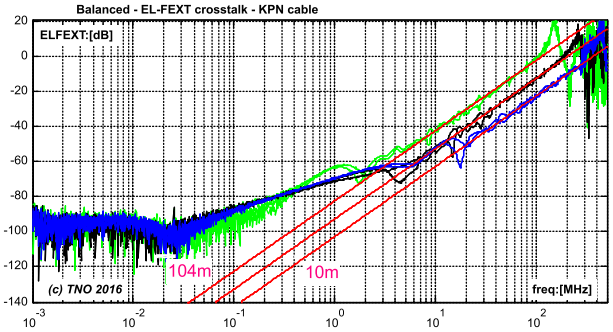

Fig. 15. Measured EL-FEXT on quad "A", at three loop lengths ($L = 104$, 32 and 10 m). The straight lines (40 dB/decade) for each of these lengths are defined as $K_{XF2} \cdot (L/L_0) \cdot (\omega/\omega_0)^2$, where $K_{XF2} = -63$. dB The good match between measurements and lines demonstrate the linear dependency on the loop length.

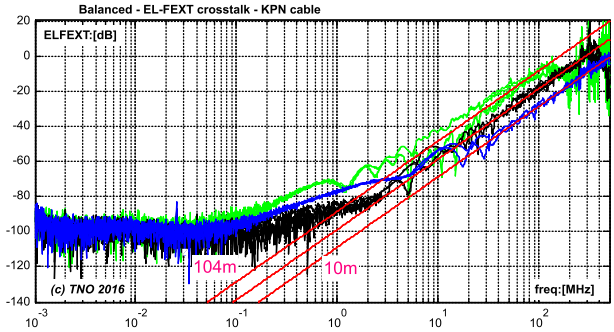

Fig. 16. Measured EL-FEXT on quad "B", at the same loop lengths as in figure 15. The twist length of this quad "B" is half of quad "A" and therefore the straight lines are drawn 6 dB below those of figure 15 ($K_{XF2,b} = -68\,dB$). The good match with this 6 dB demonstrates the linear dependency on the twist length.

length (one of 104, 32 or 10 m), $L_0 = 1000,\mathrm{m}$ $\omega_0 = 2\pi \cdot 1\,\mathrm{MHz}$ and $K_{XF2} = -63\,\mathrm{dB}$ These three straight lines scale proportionally with the loop length and fit very well with the measured EL-FEXT values where their second order effect dominates (above 5 MHz for the longest loop). This validates our prediction in section VI on loop length dependency.

In addition, these measurements show that the first order EL-FEXT is a bit random in nature and that shorter loops can sometimes have higher EL-FEXT values then longer loops. The well-known length dependency of the first order effect (proportionally with $\sqrt{L}$) holds therefore only in a statistical sense. Furthermore, the "resonating" behavior around 0 dB is quite different for each length. This looks as random, but our deterministic model can predict a similar behavior.

All the six quads in our cable have different twist lengths, and we observed values ranging from 4 to $10.5\,cm$ in this cable. The above quad "A" had a twist length of about $10 \sim 10.5\,cm$, and we also measured an adjacent quad "B" having a twist length of about $5 \sim 5.5\,cm$. Their twist length differ a factor 2, while all other aspects are similar to that of quad "A". Our model predicts in section V-A that the second order EL-FEXT in quad "B" should therefore be about 6 dB lower than in quad "A".

Figure 16 shows the two (forward) in-quad EL-FEXT curves of quad "B", for all three loop lengths, as well as the straight lines defined above. The difference is that those straight lines are now drawn exactly 6 dB lower than for quad "A", so $K_{XF2,b} = -69\,dB$. Again the measured EL-FEXT values match these lines very well where their second order effect dominates. This 6 dB difference validates our prediction in section V-A on twist length dependency.

Figure 17 shows an EL-FEXT measurement within an unshielded twisted quad telephony cable, as described in section 4 of [6]. At a first glance the figure validates our prediction that only the first order slope (20 dB/decade) will be present in unshielded quad cables. However, such cables are often low-quality cables, and that explains why the EL-FEXT near 10 MHz is in figure 17 about $20\,dB$ higher than the values shown in figure 15 and 16. So one can also claim that the first order effect dominates in this particular cable the second order crosstalk. As a result, the validation of this

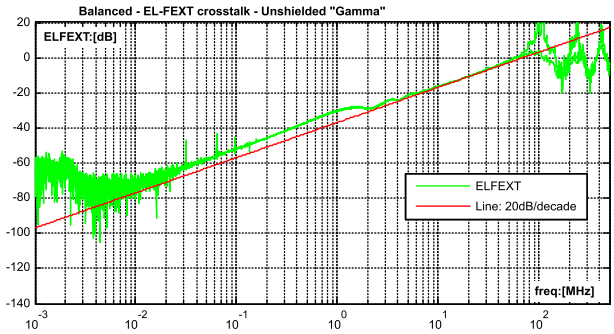

Fig. 17. Measured EL-FEXT on quad "B", at the same loop lengths as in figure 15. The twist length of this quad "B" is half of quad "A" and therefore the straight lines are drawn 6 dB below those of figure 15 ($K_{XF2,b} = -68\,dB$). The good match with this 6 dB demonstrates the linear dependency on the twist length.

prediction remains inconclusive and we leave such a validation as for future work.

VIII. Simplified EL-FEXT Model

For system performance calculations on DSL systems, the brute force approach of our model is a bit overkill. Therefore a simplified approximate model of EL-FEXT as function of the frequency and of the cable may be preferred in these cases. This means the use of a simple transfer function $H_{ELFEXT}(j\omega, L)$, to approximate the magnitude of the EL-FEXT as function of frequency and cable length L.

The legacy model [10], [11] using that approach is a first order transfer function and is too simple for higher frequencies. The model in [21]:sect A.2.3.1 with just two straight lines is also too simple since it ignores that those two lines scale differently with the cable length. It also ignores that the EL-FEXT cannot keep growing to infinite high values for increasing frequencies. Therefore we refined our previous approach in [5], which is based on a transfer function description of second order high-pass filters in general.

The second order transfer function in equation 6 can model the magnitude of EL-FEXT curves much better, since it (a) supports both the first and second order slope, has (b) an asymptotic limitation for higher frequencies at 0 dB, scales

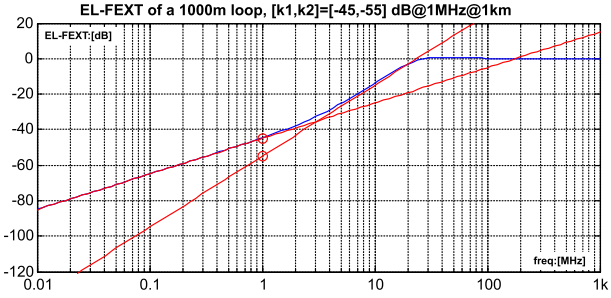

Fig. 18. Result from the simplified EL-FEXT model for a 1000 m loop, when $K_{XF1} = -45$ dB and $K_{XF2} = -55$ dB. The blue curve is the model, the red lines are its asymptotes $k_1 \cdot (\omega/\omega_0)$ and $k_2 \cdot (\omega/\omega_0)^2$. They cross each other near 3.3 MHz. The markers at 1 MHz through these asymptotes are representing the values K_{XF1} and K_{XF2}.

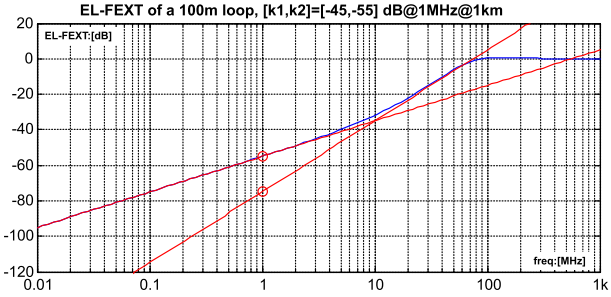

Fig. 19. Result from the simplified EL-FEXT model for a 100 m loop, when $K_{XF1} = -45$ dB and $K_{XF2} = -55$ dB. The blue curve is the model, the red lines are its asymptotes $k_1 \cdot (\omega/\omega_0)$ and $k_2 \cdot (\omega/\omega_0)^2$. They cross each other near 10 MHz.

(c) the first order slope with the root of the cable length and scales (d) the second order slope linearly with the cable length. The transfer function is defined in such a manner that the overshoot near 0 dB is insignificant.

$$H_{ELFEXT}(j\omega, L) = \left\| \frac{k_1(L) \cdot \left(\frac{j\omega}{\omega_0}\right) + k_2(L) \cdot \left(\frac{j\omega}{\omega_0}\right)^2}{1 + \left(k_1(L) + \sqrt{k_2(L)}\right) \cdot \left(\frac{j\omega}{\omega_0}\right) + k_2(L) \cdot \left(\frac{j\omega}{\omega_0}\right)^2} \right\| \quad (6)$$

where $k_1(L) = K_{XF1} \cdot \sqrt{L/L_0}$, and $k_2(L) = K_{XF2} \cdot (L/L_0)$.

In this expression, ω_0 and L_0 are arbitrary scaling constants (e.g. 1 MHz and 1 km), and K_{XF1} and K_{XF2} are empirical values for matching the EL-FEXT characteristics between particular wire pairs of interest. To model our example cable, values like $K_{XF1} = -68.2$ dB and $K_{XF2} = -76.6$ dB, both normalized to 1 MHz and 1 km cable, are adequate. When $K_{XF2} = 0$ this enhanced model approximates the legacy model for EL-FEXT, since K_{XF1} is usually <<1.

Figure 18 and 19 illustrate how the formula of the simplified EL-FEXT model behaves for different loop lengths. The red lines, specified by $k_1 \cdot (\omega/\omega_0)$ and $k_2 \cdot (\omega/\omega_0)^2$, are the asymptotes of these blue curves. The asymptote raising with 20 dB/decade scales proportionally with the root of the loop length L, since $k_1(L) = K_{XF1} \cdot \sqrt{L/L_0}$. The asymptote raising with 40 dB/decade respectively, scales proportional with the loop length L, because $k_2(L) = K_{XF2} \cdot (L/L_0)$. They cross each other near 3.3 MHz for the 1000 m loop and near 10 MHz for the 100 m loop. The blue line is limited near 0 dB so the blue curve has the desired behavior over the full frequency band. When adequate values for K_{XF1} and K_{XF2} are found to match a particular cable of interest, the simplified model offers a fair description of the EL-FEXT over a wide range of frequencies and loop lengths.

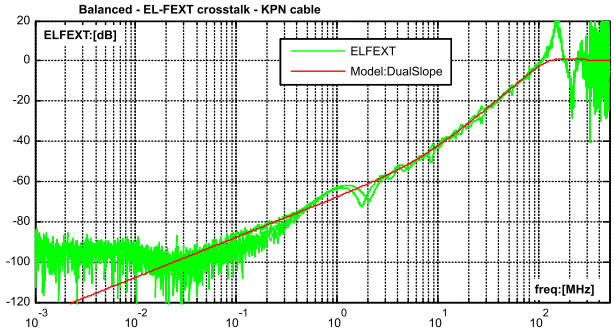

Fig. 20. Match between the EL-FEXT measurements shown in figure 15 for 104m of quad "A" and our simplified EL-FEXT model ($K_{XF1} = -58$ dB and $K_{XF2} = -64$ dB). In spite of its simplicity, it offers a good match over a wide frequency interval up to the frequency where the model crosses 0 dB.

Figure 20 shows how close this model can match real measurements, applied to one of them from section VII.

IX. Conclusions

It is well-known that the ratio between received crosstalk and received signal level in telephony cabling increases with the frequency, but the awareness that the increase of the in-quad EL-FEXT becomes much stronger above a certain frequency (40 dB instead of 20 dB per decade) was raised only recently [5], [12]. This increase puts strong demands on vectoring engines of DSL modems to let VDSL and G.fast make efficient use of higher frequencies. We elaborated on a full-8-port model of four wires in a quad, to quantify various characteristics of this dual slope behavior of in-quad EL-FEXT in these cables.

Our model demonstrates that the first order and second order effects in in-quad EL-FEXT scale differently with the cable length. The well-known first order effect originates from random perturbation of the geometry, scales proportionally with the root of the cable length (in a statistical sense) and offers the EL-FEXT its slope of 20 dB/decade.

The second order effect is deterministic in nature. It occurs when the metallic surroundings of two wire pairs in a quad (e.g. a shield) disturb the balance of a perfect quad structure. Twisting the quad can reduce this effect significantly but a residue will always remain. This residue contributes a slope of 40 dB/decade to the in-quad EL-FEXT, and can dominate the first order effect above a certain frequency. It proceeds until the in-quad EL-FEXT approaches 0 dB. The magnitude will then meander with rapid variations around 0 dB.

Our model also quantifies how this second order effect scales with various design parameters of the cable. It shows that (a) an increase of twist length by a factor 10 will increase this effect by 20 dB, (b) an increase of shield unbalance by a

factor 10 will increase it by 40 dB, and (c) an increase of the average capacitance to shield will also increase it significantly but that effect is not linear.

We validated the predictions of our model that this second order EL-FEXT scales linearly with the cable length as well as with the twist length.

The improved understanding of this second order crosstalk effect brought us to propose a simplified but adequate model of in-quad EL-FEXT [10], [11] for supporting system calculations on the performance of DSL systems. This takes more aspects into account than the simple model with two-lines described in [21].

ACKNOWLEDGMENT

The author would like to thank Jeroen Boschma from TNO for his assistance with all the cable measurements, as well as the Editor and anonymous reviewers for their input.

REFERENCES

[1] P. Odling, T. Magesacher, S. Host, P. O. Borjesson, M. Berg, and E. Areizaga, "The fourth generation broadband concept," *IEEE Commun. Mag.*, vol. 47, no. 1, pp. 62–69, Jan. 2009.

[2] *Self-FEXT Cancellation (Vectoring) for Use With VDSL2 Transceivers*, document ITU-T G.993.5, ITU-T, 2015.

[3] *Fast Access to Subscriber Terminals (FAST)—Power Spectral Density Specification*, document ITU-T G.9700, ITU-T, 2014.

[4] *Very High Speed Digital Subscriber Line Transceivers 2 (VDSL2)*, document ITU-T G.993.2, ITU-T, 2015.

[5] R. F. M. van den Brink, *G.fast: Dual Slope Behaviour of EL-FEXT*, document TNO Contribution 2012-02-4A-038 to ITU-T SG15/Q4, Feb. 2012.

[6] R. F. M. van den Brink, J. Boschma, and M. Popova, *G.fast: Wideband Transfer and Crosstalk Measurements on Twisted Pair Cables*, document TNO Contribution 11BM-021 to ITU-T SG15/Q4, Apr. 2011.

[7] R. F. M. van den Brink, *G.fast: Wideband Modeling of Twisted Pair Cables as Two-Ports*, document TNO Contribution 11GS3-028 to ITU-T SG15/Q4, Sep. 2011.

[8] T. Magesacher, "MTL—A multi-wire transmission line modeling toolbox," *J. Comput. Elect. Eng.*, vol. 5, no. 1, pp. 52–55, Feb. 2013.

[9] D. Acatauassu, S. Höst, C. Lu, M. Berg, A. Klautau, and P. O. Börjesson, "Simple and causal copper cable model suitable for G.fast frequencies," *IEEE Trans. Commun.*, vol. 62, no. 11, pp. 4040–4051, Nov. 2014.

[10] *Spectral Management on Metallic Access Networks; Part 2: Technical Methods for Performance Evaluations*, document ETSI TR 101 830-2, Rev. V1.2.1, ETSI, 2008.

[11] Bell Telephone Laboratories, *Transmission Systems for Communications*, 4th ed. Holmdel, NJ, USA: Bell Telephone Labs, 1971.

[12] R. F. M. van den Brink, *G.fast: Far-End Crosstalk in Twisted Pair Cabling; Measurements and Modelling*, document TNO Contribution 11RV-022 to ITU-T SG15/Q4, Nov. 2011.

[13] P. Eriksson, M. Berg, and C. Lu, *G.fast: Equal-Length FEXT Measurements on PE05 Cable*, document Ericsson Contribution 11RV-054R1 to ITU-T SG15/Q4, Richmond, VA, USA, Nov. 2011.

[14] *G.fast: Equal-Length FEXT Measurements on PE05 Cable*, document Huawei Contribution COM 15-C 1864 to ITU-T SG15/Q4, Nov. 2011.

[15] D. Bruyssel and J. Maes, *G.fast: Dual Slope Behaviour of EL-FEXT*, document ALU Contribution 2012-06-4A-033 to ITU-T SG15/Q4, May 2012.

[16] L. Humphrey, *On Dual Slope FEXT Observations*, document BT Contribution 2012-05-4A-021 to ITU-T SG15/Q4, May 2012.

[17] L. Humphrey and Morsman, *G.fast: FEXT Cable Measurements*, document BT Contribution 2012-05-4A-025 to ITU-T SG15/Q4, May 2012.

[18] P. Muggenthaler and C. Tudziers, *G.fast: EL-FEXT Analysis*, document DT Contribution 2012-06-4A-041 to ITU-T SG15/Q4, May 2012.

[19] T. Bongard, *G.fast: Dual Slope ELFEXT Behaviour on Swiss Cables*, document Swisscom contribution 2013-01-Q4-042 to ITU-T SG15/Q4, Feb. 2013.

[20] K. Schneider, K. Kerpez, T. Starr, and M. Sorbara, "Transfer functions, input impedance and noise models for the loop end," unpublished.

[21] *Broadband Copper Cable Models, Issue 1*, document TR-285, BBF, Feb. 2015.

[22] *Broadband Copper Cable Models, Issue 1, Corrigendum 1*, document TR-285, BBF, Nov. 2015.

[23] A. Kozarev, R. Strobel, S. Leimer, and P. Muggenthaler, *Modeling of Twisted-Pair Quad Cables for MIMO Applications*, document Lantiq/DT Contribution bbf2014.467 to Broadband Forum, (Updated From bbf2014.377 and bbf2014.117), Jun. 2014.

[24] R. Strobel, R. Stolle, and W. Utschick, "Wideband modeling of twisted-pair cables for MIMO applications," in *Proc. Symp. Sel. Areas Commun. (GLOBECOM)*, Dec. 2013, pp. 2828–2833.

[25] R. F. M. van den Brink, *Understanding and Modelling the Dual Slope Effect on EL-FEXT*, document TNO Contribution 2016-04-Q4-021 to ITU-T SG15/Q4, Apr. 2016.

[26] R. F. M. van den Brink, *Understanding the Dual-Slope Effect in Crosstalk (EL-FEXT)*, document TNO Contribution bbf2016.685 to Broadband Forum (WT-285), Jul. 2016.

[27] R. F. M. van den Brink, *Modeling the Dual-Slope Behavior of In-Quad EL-FEXT in Twisted Pair Quad Cables*, document TNO Contribution bbf2016.686 to Broadband Forum (WT-285), Jul. 2016.

[28] R. F. M. van den Brink, *A Simplified EL-FEXT Model, Addressing the Dual Slope Effect and Its Length-Dependency*, document TNO Contribution bbf2016.687 to Broadband Forum (WT-285), Jul. 2016.

[29] R. F. M. van den Brink, *Enabling 4GBB Via Hybrid-FTTH, the Missing Link in FTTH Scenarios*, document TNO Contribution bbf2010.1395 to Broadband Forum, Dec. 2010.

[30] C. R. Paul, *Analysis of Multiconductor Transmission Lines*. Hoboken, NJ, USA: Wiley, 2008.

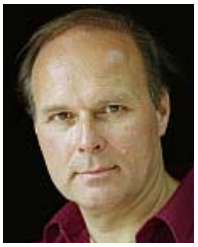

Rob F. M. van den Brink received the degree in electronics from the Delft University of Technology in 1984, and the Ph.D. degree in 1994. He is a Senior Scientist with TNO, with a focus on broadband access networks. Since 1996, he has played a very prominent role in DSL standardization in (ETSI, FSAN). He has written over 100 technical contributions to ETSI, and several contributions or ITU and BBF. He took the lead within ETSI-TM6 in identifying/defining cable models, test loops, noise models, performance tests, and spectral management. He is an Editor of an ETSI-TM6 reference document on European cables, and led the creation of the MUSE Test Suite, from 2004 to 2008, a comprehensive document for analyzing access networks as a whole. He also designed solutions for spectral management policies in The Netherlands, and created various DSL tools for performance simulation (SPOCS), cable modeling (TICAM), and noise generation for testing that are currently in the market. He has been Rapporteur/Editor of ETSI since 1999 (on Spectral Management: TR 101 830), a Board Member of the MUSE consortium from 2004 to 2008. Since 2009, he is a Work Package Leader within various projects of the Celtic 4GBB Consortium. This consortium received three awards for the initiation the development and standardization of G.fast.